# A large area detector with indirect conversion, charge integration and photon counting operation

Becker, B., Kaercher, J., Krug, M., Leo, S., Stuerzer, T., et al.

B. Becker, J. Kaercher, M. Krug, S. Leo, T. Stuerzer, B. Weinhausen, R. Durst, "A large area detector with indirect conversion, charge integration and photon counting operation," Proc. SPIE 11838, Hard X-Ray, Gamma-Ray, and Neutron Detector Physics XXIII, 118380N (1 September 2021); doi: 10.1117/12.2597029

SPIE.

Event: SPIE Optical Engineering + Applications, 2021, San Diego, California, United States

# A large area detector with indirect conversion, charge integration and photon counting operation

B. Becker[1], J. Kaercher[1], M. Krug[2], S. Leo[2], T. Stuerzer[2], B. Weinhausen[2], R. Durst[2*]

[1]Bruker AXS Inc., 5465 E Cheryl Parkway, Madison, WI 53711, USA
[2]Bruker AXS GmbH, Östliche Rheinbrückenstraße 49, 76187, Karlsruhe, Germany
*Corresponding author.

## Abstract

A new large-area pixel detector for X-ray diffraction combining indirect conversion with charge integration and photon counting is described. Indirect conversion achieves a large active area with no gaps or dead areas and also a high Detective Quantum Efficiency across the energy range of interest for X-ray diffraction, from 6 keV to 24 keV. The detector runs in charge integration mode which allows photon counting with no counts lost to charge sharing or coincident pulse effects. The detector is also able to discriminate against high energy events from the natural background radiation which allows the acquisition of very long exposures with essentially zero noise.

## Keywords

X-ray detection, photon counting, indirect detection, charge integration.

## Introduction

Hybrid Photon Countering X-ray detectors (HPCs) have found increasing use in many scientific applications including X-ray diffraction. In an HPC, an X-ray photon is absorbed in a semiconductor sensor to produce a charge cloud via photoionization[1]. The voltage signal produced by this charge is then amplified and compared to a threshold in a hybridized ASIC. If the signal exceeds the threshold it is counted, if not it is rejected as noise.

For example, HPCs have become the detector of choice for many synchrotron applications due to their high-count rate capability combined with single photon sensitivity[2]. They are also suitable for many laboratory applications, especially those that require long exposure times such as, for example, Small Angle X-Ray Scattering (SAXS) because they do not accumulate detector noise and thus can take very long exposures.

However, it is known that conventional HPC detectors also suffer from shortcomings which have limited their application in other areas. Firstly, HPC detectors, despite being true digital detectors suffer from a new type of noise due to charge sharing[3]. That is, when X-rays are absorbed near a pixel boundary the charge is shared between two or more pixels which leads to the loss of counts when the divided signal is compared to a simple binary threshold. It has recently been shown that this effect can significantly degrade data quality in crystallographic experiments[4]. Secondly, conventional HPC detectors suffer from coincident events or pulse pileup which limits their instantaneous count rate capability. That is, when two or more X-rays hit a given pixel simultaneously, a conventional HPC will only record a single event, leading to loss of signal[4]. This is especially important for pulsed X-ray applications such as, for example, X-ray Free Electron Lasers.

To mitigate these limitations, a new generation of pixel array detectors has been recently developed based on charge integration. These detectors include, for example, the JUNGFRAU detector[5], and the AGIPD detector[6].

These charge-integrating pixel array detectors use a semiconductor hybrid sensor as in an HPC. However, instead of comparing the signal produced by an X-ray to a simple binary threshold, these charge integrating detectors integrate the

Hard X-Ray, Gamma-Ray, and Neutron Detector Physics XXIII, edited by Nerine J. Cherepy
Michael Fiederle, Ralph B. James, Proc. of SPIE Vol. 11838, 118380N · © 2021 SPIE
CCC code: 0277-786X/21/$21 · doi: 10.1117/12.2597029

charge produced by the X-rays incident on the detector during a short (on the order of msec) exposure time. Photon counting can then be achieved in such a detector by locating and counting single X-ray events in the individual frames[5].

This charge integration approach has two key advantages compared to conventional HPC detectors[5]. First, if an X-ray is absorbed near a pixel boundary, then the charge will be divided between the neighboring pixels, exactly as in an HPC. However, in a charge integrating pixel detector, all the charge is recorded and the photon counting processor can thus combine the charge in adjacent pixels and properly count the event[5]. Thus, unlike an HPC, a charge integrating pixel detector does not suffer from charge sharing noise. Secondly, if more than one X-ray hits a pixel during a frame, the accumulated charge from multiple X-rays is stored and can thus be properly counted as two (or more) X-rays. Thus, coincident event or pulse pileup noise is also eliminated[5].

Recently, the latest generation of HPC and charge integrating pixel array detectors have been compared directly and it has been shown experimentally that charge integrating detectors can produce significantly superior data in real X-ray diffraction experiments. For example, Leonarski et al. compared the crystallography R-factor and anomalous signal versus resolution for a Thaumatin crystal measured using an HPC (EIGER) and a charge integrating pixel array detector (JUNGFRAU) [7]. It was found that the JUNGFRAU data were significantly superior due to the elimination of charge sharing noise and pulse pileup.

## Charge-integrating detectors with indirect detection

The JUNGFRAU and AGIPD charge-integrating pixel array detectors described above employ a hybridized semiconductor sensor, like conventional HPC detectors. However, recently it has been proposed that it is possible to implement this charge integration/photon counting approach with an indirect detector, that is, with a scintillator converter rather than a semiconductor sensor.

As noted above, in an HPC an X-ray is absorbed in a semiconductor, thus producing electron-holes pairs which are detected by the counting electronics. In an indirect detector, the X-ray is absorbed in a scintillator which then emits visible photons. These visible photons are then detected using a pixel array in which each pixel incorporates a photodiode.

The challenge of an indirect photon-counting detector is that the quantum gain from a scintillator is significantly lower than in a semiconductor. For example, when an 8.1 keV X-ray (Cu K$\alpha$) is absorbed in silicon, it produces on the order of 2200 electron-hole pairs. In contrast, in a scintillator screen the same X-ray typically produces on the order of 100-200 photons[8].

Despite this, photon-counting detectors using indirect detection are, of course, well known in the scientific literature. In particular, the combination of a scintillator with a photomultiplier tube (PMT) has long been used for X-ray photon counting in a broad range of applications. In a PMT-based photon counter, the relatively low quantum gain of the scintillator is compensated by the near-zero electronic noise of the photo multiplier tube to allow single photon counting.

Recently very low noise CMOS pixel arrays have become available with noise on the order of 10 electrons or less. Using such very low noise pixel arrays the signal-to-noise ratio for a single X-ray event detected by a scintillator is higher than 10 which is high enough for photon counting. It is thus now possible in principle to achieve charge integration with photon counting with an indirect (scintillator) detector, exactly as in the latest generation direct (semiconductor) charge integrating pixel detectors.

For example, Dierickx et al described an indirect photon-counting detector based on a novel pixel array with noise on the order of 10 electrons per pixel RMS[9]. Similarly, Nishihara et al described an indirect photon counting detector based on a scintillating convertor coupled to a new pixel array sensor with a noise of less than 1 electron per pixel RMS[10].

These authors point out that the use of indirect detection with a photon-counting pixel area detector has several potential advantages. For one thing, it is possible to produce an indirectly-coupled detector with a large active area (hundreds of $cm^2$) with no gaps or dead areas. It is currently not possible to do this with hybridized semiconductor detectors. This is a crucial advantage in certain applications, for example, in medical radiography where dead gaps in an image could miss incipient malignancies.

Another advantage of indirect detectors is that they have relatively high effective atomic numbers and thus can achieve efficient X-ray absorption over a broad energy range. For X-ray diffraction the typical energy range of interest is from Cr Kα (4.9 keV) up to In Kα (24 keV). Using a scintillator it is possible to achieve better than 90% X-ray absorption across this entire energy range.

In contrast, most HPC designs rely on silicon as the sensor element. This works well at lower energies, however, at energies higher than about 15 keV Si absorption is fairly low. For example, for a 300 µm thick Si sensor the absorption at Ag Kα (22.2 keV) is only 20%. Absorption may be improved by using a thicker Si sensor but even with a 600 µm thick sensor absorption is only improved to 37%.

Also, when using such a thicker Si sensor at large angles of incidence, the signal suffers from parallax which causes the X-ray signal to be 'smeared'. For example, in the case of a 600 µm thick Si sensor, when X-rays hit the detector at an oblique angle of 45 degrees then a nominally round Bragg reflection of 100 µm diameter will by smeared into a 100 µm x 600 µm ellipse. This so-called parallax effect significantly degrades the spatial resolution at high incident angles which can cause overlap of adjacent Bragg reflections.

The other approach to improving the absorption of HPCs at higher energy is to use CdTe or a similar high atomic number compound semiconductor as the sensor element. For example, a 300 µm thick CdTe sensor can achieve high absorption (>90%) across the energy range of interest for X-ray diffraction. However, CdTe is significantly more expensive per unit area than Si which limits its economic viability for large area detectors.

As noted above, conventional scintillators such as, for example, Gd2O2S:Tb or CsI:Tl are able to achieve high absorption across the 6-24 keV energy range (>90%), similar to CdTe but at a significantly lower cost per unit area and without the parallax effect suffered by thicker Si sensors.

The response of these scintillators is also extremely temporally stable and reproducible. This is not necessarily true of all semiconductor sensors, especially compound semiconductors such as CdTe which can suffer from quantum gain drifts due to polarization[11].

The spatial resolution of an indirect detector as quantified by the Point Spread Function or equivalently, the Modulation Transfer Function, is degraded by light scattering in the scintillator screen. The lack of such scattering in a direct detector is often cited as one of their key advantages. However, Nishihara pointed out that in a photon-counting indirect detector, if the signal spans more than one pixel it is possible to measure the centroid of the light cloud produced by each X-ray. Thus, it is possible to measure the centroid of the light cloud with a precision smaller than the pixel size. Nishihara thus showed that an indirect detector could achieve a Modulation Transfer Function of 0.8 at 10 line pairs per millimeter, comparable to, or even better, than the best resolution reported for direct HPCs[10].

## The PHOTON III – an indirect detector with charge integration and photon counting

The PHOTON III, shown in Figure 1, is a new detector which was designed for X-ray diffraction and implements the charge integration approach with indirect detection, like the detectors described by Dierickx and Nishihara above. We believe that it is the first commercially available detector to implement this approach.


Figure 1. PHOTON III detector

The operating characteristics for the PHOTON III are shown in Table I.

| | |
|---|---|
| Active area | Up to 240x100 $mm^2$ |
| Pixel size | 135 µm |
| Gaps, dead areas | None, 100% of detector surface fully sensitive to X-rays |
| Conversion | Indirect |
| Conversion quantum gain | 25 electrons/keV |
| Electrical noise | <10 electrons |
| Energy range | 8-24 keV |
| Detective Quantum Efficiency | >90% |
| Frame rate | 70 to 140 Hz max |
| Dynamic range (1 sec exposure) | Up to 420,000 X-rays (Cu Ka) |
| Point spread function (FWHM) | <90 µm |
| Parallax | <1 pixel |
| Stability | <0.1% variation in response over 1 hour |
| Linearity | <1% deviation over full range |
| Cosmic ray rejection | >99.99% of cosmic ray signals eliminated |
| Charge sharing noise | None, 0% of pixel area lost due to charge sharing |

Table I. Operating characteristic of the PHOTON III.

Indirect detection allows the PHOTON III to achieve a large active area (currently up to 240 $cm^2$) without gaps or dead areas. The scintillator has a high Detective Quantum Efficiency (DQE) across a broad range on energies (>90% from 8-24 keV) without significant parallax (less than one pixel).

The PHOTON III is based on a proprietary active pixel sensor manufactured by Teledyne Dalsa (www.teledynedalsa.com). The three-side buttable sensor features a pixel size of 135 µm x 135 µm, an active area of up to 140 x 100 $mm^2$, a pixel fill factor of 85%, and a total noise of <10 electrons.

Running in charge-integrating mode, for a single Cu Kα X-ray, the PHOTON III is thus able to achieve a signal-to-noise ratio of over 20 which is sufficient for true single photon counting.

The PHOTON III runs at frame rates of up to 140 Hz (7 msec minimum frame time) in rolling shutter mode. The detector typically runs at the maximum possible frame rate, even when the desired integration time is longer than 7 msec. Each of these fast frames is then searched for photons in real time using a pipeline processor (FPGA). Figure 2 shows a single exposure showing the detection of single X-rays. The red circles show the X-ray locations identified by the processor.

If two or more X-rays are absorbed in a single pixel during a frame integration, then the processor will interpret this properly as a multiple X-ray event and thus counts are not lost due to pulse overlap as in conventional HPCs. Also, the processor can 'see' X-rays that are absorbed near a pixel boundary and thus are shared between adjacent pixels. Thus, these shared events are properly counted and there are no charge sharing losses.

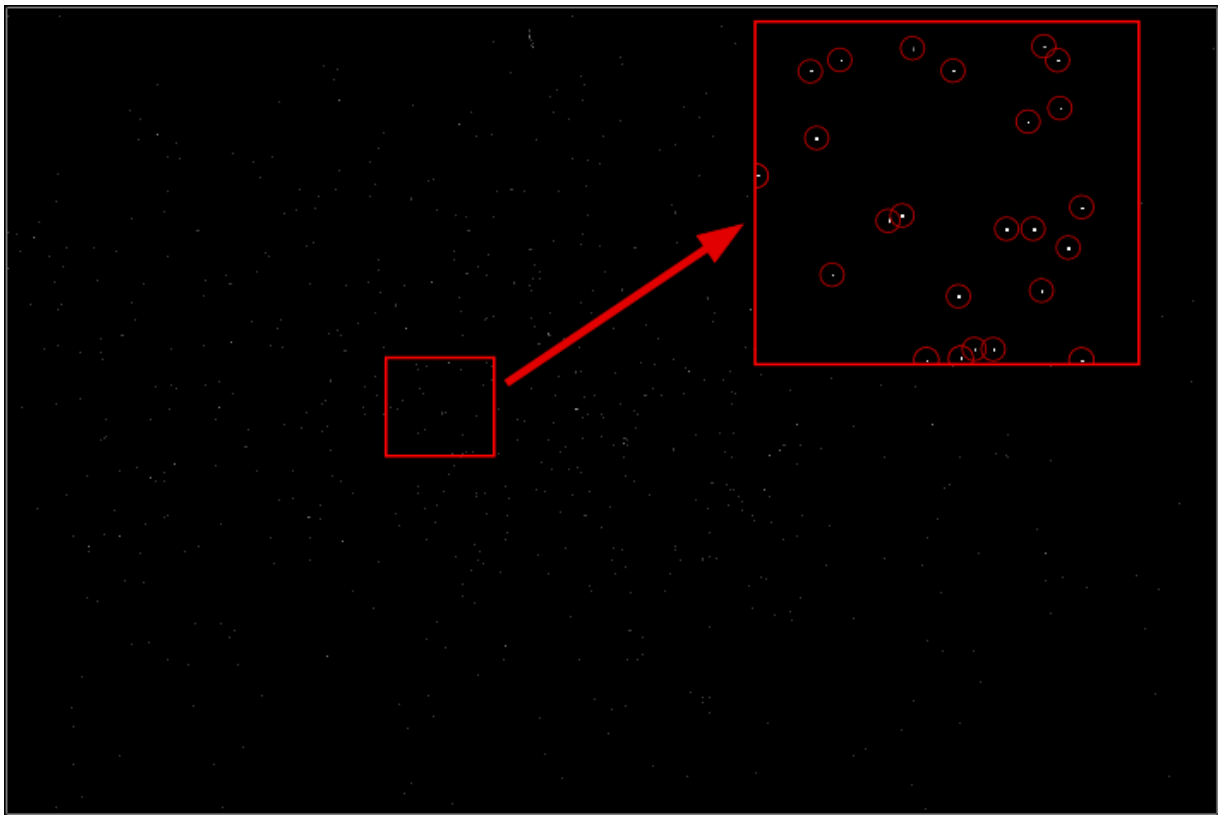

Figure 2. A single fast exposure showing diffracted X-rays captured with the PHOTON III. The area in the red square is enlarged for clarity. The red circles show X-rays identified by the real time processor.

The PHOTON III detector employs a dual port buffer memory. Therefore, there is zero dead time between frames. This is a significant advantage during 'shutter free' data acquisition where the readout deadtime leads to gaps in the measured crystallographic rocking curve, thus reducing data quality.

In a typical diffraction experiment the integration times are on the order of seconds or even minutes. Therefore, in typical operation a series of fast frames are combined to create longer composite frames. For example, if the user requests a 1 second exposure the detector would combine 70 to 140 individual frames. Note that, since each individual fast frame is noise free, the combined composite frame is also noise free. Figure 3 shows such a one second composite image for the same sample as shown in Figure 2.

Figure 3. A 1 second composite exposure obtained by summing 70 individual exposures (diffraction from the same sample as in Figure 2). Individual Bragg reflections can be seen in the composite image. Note that at high resolution, where there are few scattered X-rays there is essentially no background noise in the composite image.

As noted above, operating a direct detector in charge-integrating mode with photon-counting conveys two key advantages: namely, it is possible to achieve true single-photon detection while also eliminating both charge sharing noise and pulse pileup. These advantages are equally valid for the PHOTON III detector operated in charge integration mode.

The dynamic range of the detector is defined as the strongest signal that can be measured normalized by the weakest signal[12]. In photon counting detector the weakest detectable signal is of course a single X-ray. In any charge-integrating detector, the maximum signal that can be measured is limited by the full well capacity of the sensor. The full well capacity depends on the electronic gain of the sensor which is software selectable between high and low gain modes. The full well capacity of the PHOTON III sensor is $160 \times 10^3$ electrons per pixel in high gain mode and $600 \times 10^3$ electrons per

pixel in low gain mode. Therefore, in each pixel the detector can store between 800 X-rays (Cu Kα) per pixel in high gain mode or 3000 X-rays per pixel in low gain mode in a single exposure.

However, an integrating detector can combine multiple frames to increase the effective dynamic range of the detector[13]. For example, if two images are summed together then the effective dynamic range is twice the dynamic range of a single exposure. This summing operation can be repeated multiple times to achieve dynamic range much higher than could be achieved in a single exposure.

This dynamic range extension principle is employed in the PHOTON III. That is, as noted above, the detector combines multiple frames in order to produce a composite frame with a higher effective dynamic range than is achieved in the constituent sub-frames. For example, typically a 1 second exposure would consist of a composite image composed of up to 140 frames summed together, which increases the effective storage of up to 112,000 X-rays/pixel (Cu Kα) in high gain mode and thus an effective dynamic range of 112,000. Similarly, it is also possible to combine sub-frames collected in both high gain and low gain modes in order to increase the effective dynamic range further, up to 420,000 X-rays per pixel for a one second exposure.

## High energy event discrimination

One of the great advantages of a photon-counting detector is that it can take very long exposures when needed because there is no detector noise. However, for long exposures, spurious signals from the natural background radiation (so-called 'zingers') can become the dominant noise source. The source of this background noise is cosmic rays and radioactive elements in the immediate environment. For this reason, the PHOTON III incorporates a high-energy event discrimination filter (HEED) to remove the noise contribution from such background radiation. Cosmic rays and natural background radiation have a distinct signature which can be used by the real time processor to distinguish between real signal from diffracted X-rays and these zinger events[14].

Figure 4 below shows an example of an exposure of 10 minutes with and without this High Energy Event Discrimination filter. For a long exposure the contribution from environmental radiation can be significant but the HEED filter reduces this effect to near zero.

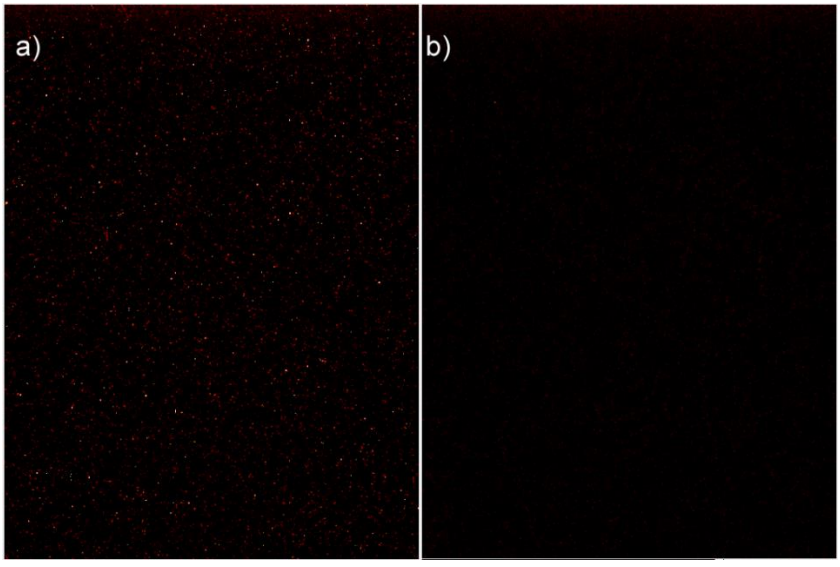


Figure 4. A 10 minute dark frame captured in photon counting mode without (a) and with (b) High Energy Event Discrimination. After several minutes of exposure, noise begins to accumulate due to the natural radiation background. For long exposures (a few minutes and longer) the contribution of the radiation background can become the dominant source of noise in the experiment. The application of High Energy Event Discrimination nearly eliminates this source of noise.

## Data comparisons

Figure 5 shows a diffraction frame collected in charge integrating with photon counting. The application of photon counting essentially eliminates detector noise, allowing extremely weak signals to be measured with significantly higher precision. Table II shows the crystallographic data from the same crystal collected with and without photon counting.

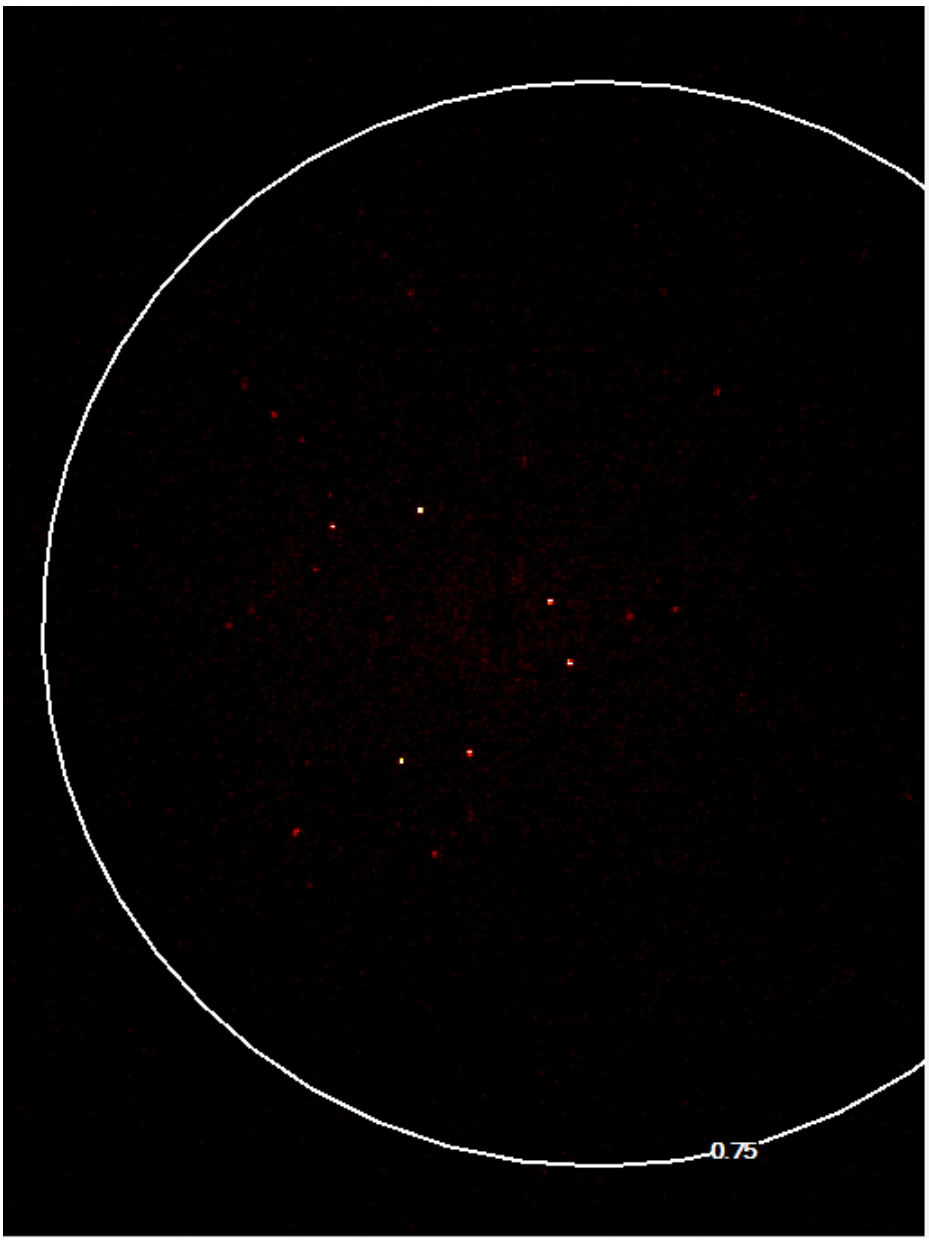


Figure 5. A 1 second crystallographic frame showing Bragg diffraction from a crystal of Cu(C5H5N)2(C7H5O3)2 collected in photon counting mode.

| | Integrating mode | Photon counting mode |
|---|---|---|
| Collection time | 8.4 min | 8.4 min |
| Exposure | 1 s | 1 s |
| Frame width | 1 deg | 1 deg |
| Resolution | 0.75 A | 0.75 A |
| Reflections | 2718 | 2705 |
| Reflections ($F_{obs} > 4\sigma(Fobs)$) | 1321 | 1865 |
| Completeness | 99.9% | 99.6% |
| Multiplicity | 7.8 | 7.7 |
| I/sigma (Inf – 0.75Å) | 6.96 | 9.56 |
| I/sigma (0.85Å – 0.75Å) | 0.7 | 2.64 |
| R(int) | 25.46% | 10.95% |
| R(sigma) | 15.4% | 5.64% |
| R1 ($F_{obs} > 4\sigma(F_{obs})$) | 5.48% | 4.57% |
| R1 (all) | 16.2% | 7.90% |
| wR2 | 11.79% | 11.33% |
| GooF | 0.948 | 1.088 |
| Residual el. Density [e/A³] | 0.35/-0.29 | 0.38/-0.47 |

Table II. Crystallographic data statistics with and without photon counting from the sample shown in Figure 5. It can be seen that, compared to conventional (analog) integration, charge integration with photon counting significantly increases the signal-to-noise ratio (I/sigma), especially for the weaker reflections at high resolution (0.85-0.75 Å ). The quality of the crystallographic model is also significantly improved as shown by the improvement in R1.

## Summary

We describe a new photon-counting detector based on charge integration with indirect conversion. The use of a scintillator allows the detector to achieve a large active area without gaps or dead areas and also allows near-ideal Detective Quantum Efficiency (>90%) over the entire range of X-ray energies relevant for X-ray diffraction without spatial smearing due to the parallax effect.

Operating in charge-integrating mode eliminates signal loss due to charge sharing and pulse coincidence. The detector is also able to discriminate between X-rays and signal from cosmic rays and the natural radioactivity background which allows very long exposures with near zero noise.

The detector has been shown to produce superior data quality in X-ray diffraction experiments including X-ray crystallography and Small Angle X-ray Scattering.

## References

[1] M. J. Renzi, M. W. Tate, A. Ercan, S. M. Gruner, E. Fontes, C. F. Powell, A. G. MacPhee, S. Narayanan, J. Wang and R. Cuenca (2002), Review of Scientific Instruments **73**:3, 1621-1624.
[2] Hatsui, T. & Graafsma, H. (2015), IUCrJ **2**, 371-383.
[3] K. Mathieson, R. Bates, V. O'Shea, M.S. Passmore, M. Rahman, K.M. Smith, J. Watt, C. Whitehill (2002), Nuclear Instruments and Methods in Physics Research A **477**, 191–197.
[4] A. Bergamaschi , R.Dinapoli, B.Henrich, I.Johnson, A.Mozzanica, X.Shi, B.Schmitt (2011), Nuclear Instruments and Methods in Physics Research A Volume 628, Issue 1, 238-241.

[5] A. Mozzanica, M. Andrä, R. Barten, A. Bergamaschi, S. Chiriotti, M. Brückner, R. Dinapoli, E. Fröjdh, D. Greiffenberg, F. Leonarski, C. Lopez-Cuenca, D. Mezza, S. Redford, C. Ruder, B. Schmitt, X. Shi, D. Thattil, G. Tinti, S. Vetter & J. Zhang (2018), Synchrotron Radiation News, 31:6, 16-20.

[6] B. Henrich, J. Becker, R. Dinapoli, P. Goettlicher, H. Graafsma, H. Hirsemann, R. Klanner, H. Krueger, R. Mazzocco, A. Mozzanica, H. Perrey, G. Potdevin, B. Schmitt, X. Shi, A.K. Srivastava, U. Trunk, C. Youngman (2011), Nuclear Instruments and Methods in Physics Research Section A, Volume 633, Supplement 1, S11-S14.

[7] F. Leonarski, S. Redford, A. Mozzanica, C. Lopez-Cuenca, E. Panepucci, K. Nass, D. Ozerov, L. Vera, V. Olieric, D. Buntschu, R. Schneider, G. Tinti, E. Froejdh, K. Diederichs, O. Bunk, B. Schmitt , M. Wang (2018) , Nature Methods, **15**, 799-804.

[8] G. Prekas, H. Sabet, H. Bhandari, G. Derderian, F. Robertson, H. Kudrolli, C. Stapels, J. Christian, S. Kleinfelder, S. Cool, J. D'Aries, V. Nagarkar (2012), IEEE Nuclear Science Symposium Conference Record, 10.1109/NSSMIC.2011.6154354.

[9] B. Dierickx, Q. Yao, N. Witvrouwen, D. Uwaerts, S. Vandewiele, P. Gao (2016), *Sensors*, 16(6), 764.

[10] Nishihara, Toshiyuki & Baba, Hiroyasu & Matsumura, Masao & Kumagai, Oichi & Izawa, Takashi. (2019), Proc. SPIE 10948, Medical Imaging 2019: Physics of Medical Imaging, 109481U; doi: 10.1117/12.2510996.

[11] V. Astromskas, E. N. Gimenez, A. Lohstroh and N. Tartoni (2016), *IEEE Transactions on Nuclear Science*, vol. 63, no. 1, 252-258.

[12] A. Ganguly, P. G. Roos, T. Simak, J. Michael Yu, S. Freestone, D. Hondongwa, R.E. Colbeth, I.P. Mollov (2018), Proc. SPIE 10573, Medical Imaging 2018: Physics of Medical, Imaging, 105730N.

[13] E. Reinhard, W. Heidrich, P. Debevec, S. Pattanaik, G. Ward, K. Myszkowski (2010), High Dynamic Range Imaging, Elsevier, ISBN 9780123749147.

[14] H. Jiang, J. Kaercher, R. Durst (2019), *Indirect Photon-Counting Analytical X-ray Detector*, *EU Patent 3444638*.